Available online at www.sciencedirect.com
ScienceDirect
Chinese Journal of Natural Medicines 2021, **19**(11): 825-835
doi: 10.1016/S1875-5364(21)60086-9
Chinese Journal of Natural Medicines

•Research article•

Anti-anaphylactic potential of benzoylpaeoniflorin through inhibiting HDC and MAPKs from *Paeonia lactiflora*

ZHONG Wan-Chao[1Δ], LI En-Can[2Δ], HAO Rui-Rui[2], ZHANG Jing-Fang[1], JIN Hong-Tao[2, 3*], LIN Sheng[1, 4*]

[1] *State Key Laboratory of Bioactive Substance and Function of Natural Medicines, Institute of Materia Medica, Chinese Academy of Medical Sciences & Peking Union Medical College, Beijing 100050, China;*
[2] *New Drug Safety Evaluation Center, Institute of Materia Medica, Chinese Academy of Medical Sciences & Peking Union Medical College, Beijing 100050, China;*
[3] *Beijing Union-Genius Pharmaceutical Technology Co., Ltd., Beijing 100176, China;*
[4] *Key Laboratory of Chinese Internal Medicine of Ministry of Education and Beijing, Dongzhimen Hospital, Beijing University of Chinese Medicine, Beijing 100700, China*

Available online 20 Nov., 2021

[ABSTRACT] Guided by cell-based anti-anaphylactic assay, eighteen cage-like monoterpenoid glycosides (**1**−**18**) were obtained from the bioactive fraction of *P. lactiflora* extract. Among these, compounds **1**, **5**, **6**, **11**, **12**, **15**, and **17** significantly reduced the release rate of *β*-HEX and HIS without or with less cytotoxicity. Furthermore, the most potent inhibitor benzoylpaeoniflorin (**5**) was selected as the prioritized compound for the study of action of mechanism, and its anti-anaphylactic activity was medicated by dual-inhibiting HDC and MAPK signal pathway. Moreover, molecular docking simulation explained that benzoylpaeoniflorin (**5**) blocked the conversion of L-histidine to HIS by occupying the HDC active site. Finally, *in vivo* on PCA using BALB/c mice, benzoylpaeoniflorin (**5**) suppressed the IgE-mediated PCA reaction in antigen-challenged mice. These findings indicated that cage-like monoterpenoid glycosides, especially benzoylpaeoniflorin (**5**), mainly contribute to the anti-anaphylactic activity of *P. lactiflora* by dual-inhibiting HDC and MAPK signal pathway. Therefore, benzoylpaeoniflorin (**5**) may be considered as a novel drug candidate for the treatment of anaphylactic diseases.

[KEY WORDS] *Paeonia lactiflora*; Anti-anaphylactic action; RBL-2H3; HDC; MAPKs
[CLC Number] R965 **[Document code]** A **[Article ID]** 2095-6975(2021)11-0825-11

Introduction

Anaphylactic diseases induced by immediate hypersensitivity reaction is a serious health problem around the world, especially in Western countries. Anaphylaxis belongs to immediate hypersensitivity reaction and is closely related to the degranulation of immunoglobulin E (IgE)-activated mast cells [1, 2]. Various inflammatory mediators, including *β*-HEX, HIS, and other cytokines such as IL-3, IL-4, IL-5,and IL-13, etc. are rapidly released from mast cells when stimulated by antigens, which induce local inflammatory response. Thus, suppressing the activation of IgE-sensitized mast cells may be an effective way for the treatment or prevention of anaphylactic diseases.

Paeonia lactiflora root, known as an important traditional Chinese medicine (TCM) "Chi-Shao" in the *Chinese Pharmacopoeia*, has long been used as a blood circulation, anti-inflammatory, and analgesic agent for the treatment of cardiocerebrovascular and anaphylactic diseases [3]. Moreover, as the characteristic chemotaxonomic markers of the genus *Paeonia*, cage-like monoterpenoid analogues from "Chi-Shao" have drawn much attention from researchers, due to their special skeleton feature as well as biological activities like anti-hyperglycemia, anti-inflammation, anti-oxidation, anti-bacteria, anti-diabetes, anti-thrombosis, anti-tumor, and liver protection [4]. Nevertheless, the anti-anaphylactic activity and mechanism of these compounds have rarely been reported.

[Received on] 10-Feb.-2021
[Research funding] This work was supported by the National Natural Science Foundation of China (Nos: 81773996, 81773589, 500101135, and 81522050) and Beijing Natural Science Foundation (No. JQ18026).
[*Corresponding author] E-mails: jinhongtao@imm.ac.cn (JIN Hong-Tao); lsznn@126.com(LIN Sheng)
[Δ]These authors contributed equally to this work.
These authors have no conflict of interest to declare.

Our preliminary anti-anaphylactic screening results indicated that the CS-4 fraction of "Chi-Shao" water extracts remarkably reduced HIS and *β*-HEX levels on RBL-2H3 cells with less cytotoxic effects. Therefore, bioactivity-guided isolation strategy was used to explore promising anaphylactic candidates from this bioactive fraction, which resulted in the isolation of eighteen cage-like monoterpenoid glycosides Fig.1 (**1**−**18**). Subsequently, seven compounds (**1**, **5**, **6**, **11**, **12**, **15**, and **17**) were hit in the anti-anaphylaxis assay on mast cell degranulation in RBL-2H3 cells, which down-regulated HIS and *β*-HEX at the meaningful concentrations (EC_{50} < 100 μmol·L^{-1}) with low cytotoxicity. Notably, benzoylpaeoniflorin (**5**) was of interest to us for its potent inhibitory effects on HIS and *β*-HEX, with EC_{50} values of 6.34 ± 1.14 and 18.06 ± 2.10 μmol·L^{-1}, respectively. Therefore, benzoylpaeoniflorin (**5**) was selected as the prioritized compound for the study of action of mechanism. First, molecular docking simulation demonstrated that benzoylpaeoniflorin (**5**) blocked the conversion of L-histidine to HIS by occupying the HDC active site. Furthermore, benzoylpaeoniflorin (**5**) not only effectively inhibited the MAPK signaling pathway downstream proteins ERK1/2, JNK, and p38 and thereby down-regulated the production IL-3, IL-4, IL-5 and IL-13, but also mitigated the damage in the cytoskeletal and mitochondrial membrane at a relatively low concentration. Besides, the anti-anaphylactic effect of benzoylpaeoniflorin (**5**) was shown by *in vivo* assays on passive cutaneous anaphylaxis (PCA) model using BALB/c mice. In summary, this is the first report that benzoylpaeoniflorin (**5**) exhibited anti-anaphylactic activity *in vivo* and *in vitro* by dual-inhibiting HDC and MAPK signal pathway, suggesting its potential role as a novel drug candidate for anaphylactic diseases.

Materials and Methods

HDC activity

The gram-negative bacteria *Klebsiella pneumonia* (BeNa Culture Collection, Kunshan, China) was used as a source of HDC for the preliminary studies on HDC inhibition by benzoylpaeoniflorin (**5**). The activity of HDC was quantified by the amount of histamine synthesis. Briefly, *Klebsiella pneumonia* was evenly dispersed in the liquid medium containing L-histidine·HCl (pH 5.3). DMSO was diluted by the bacterial broth to a final concentration of 0.1%, and used to dissolve benzoylpaeoniflorin (**5**) to the final concentrations of 5, 25, and 100 μmol·L^{-1}. 200 μL of the bacterial broth with or without benzoylpaeoniflorin (**5**) was added into a 96-well plate. After 24 h, the bacterial culture fluid was collected and filtered to remove the bacteria. HDC activity was quantified by the relative content of HIS in the filtered supernatant. The HIS release rate was calculated as a percentage compared to the control group.

Cell culture

RBL-2H3 cell line was purchased from the Cell Resource Center of Shanghai Institutes for Biological Sciences. The cells were cultured in Minimum Essential Medium (MEM; Invitrogen, Grand Island, NY) containing 15% fetal bovine serum (FBS; Gibco, Rockville, MD), 100 U·mL^{-1} penicillin/streptomycin (Sigma). The cells were cultured in an incubator under the condition of 37 °C, 5% CO_2. The cells were passaged once in two days, with a passage ratio of 1 : 3. Experiments were carried out on cells in the logarithmic growth phase.

Cell viability assay

RBL-2H3 cell viability was assessed by MTT assay. The cells were seeded into 96-well plates (1 × 10^5 cells/mL) overnight and stimulated by anti-DNP-IgE (Sigma, MO, USA) and DNP-BSA (Alpha Diagnostics International, TX, USA), before incubation with different concentrations of the extract fractions or compounds for 24 h. Then, the supernatant was discarded, and 200 μL of serum-free MTT solution (serum-free medium: 5 mg·mL^{-1} MTT = 10 : 1) was added to each well and incubated for 4 h. 150 μL of DMSO was added into every well after discarded the supernatant, and the crystals were sufficiently shaken to dissolve. Finally, the absorbance was measured by a microplate reader (Berthold, TriStar2S LB 942, Germany) at 490 nm. The cell survival rates were expressed as percentages of the value of normal cells.

Establishment of an anti-anaphylaxis model

RBL-2H3 cells were seeded into 96-well plates (1 × 10^5 cells/mL). The cells were treated with different concentrations of extract fractions or compounds and anti-DNP-IgE (750 ng·mL^{-1}). After incubated for 24 h, the sensitized cells were washed twice with 200 μL advanced tyrode's solution (Solarbio, Beijing, China) and stimulated with DNP-BSA (1 μg·mL^{-1}) for 1 h. The supernatant was collected for subsequent determination.

Measurement of β-HEX

First, 50 μL of supernatant was added into 96-well plate, followed by the addtion of 100 μL 4-nitrophenyl-*N*-acetyl-*β*-D-aminoglycosides. Next, 1, 2-benzenedimethanol (sigma, purity: 97%, 0.342 mg·mL^{-1}) was added into the same well. 200 μL of stop solution (0.1 mol·L^{-1} $NaCO_3$/0.1 mol·L^{-1} $NaHCO_3$) was added to each well after the plate was incubated for 45 min in a 37 °C constant temperature incubator. Finally, the absorbance was measured by a microplate reader (Berthold, TriStar2S LB 942, Germany) at 405 nm. The *β*-HEX release rate was calculated as a percentage compared to the model group: Release ratio (%) = (C or M or T – B) / (M – B) × 100%; where B is the group without cells in the well; C is the group without stimulation and sample treatment; M is the stimulated group without treatment of the tested sample; and T is the stimulated group with treatment of the tested sample.

Measurement of HIS

The HIS release rate was measured by spectrofluorometric assay. First, 100 μL supernatant was added into a total-black 96-well plate before the addition of 20 μL NaOH (40 mg·mL^{-1}) and 20 μL *O*-phthalaldehyde (10 mg·mL^{-1}) into the same well. After incubated in a 37 °C constant temperature

incubator for 15 min, 20 μL stop solution (10% HCl) was added into the plate. The plate was placed on the ice for 10 min in order to stop the reaction. Then the plate was measured with a microplate reader (Berthold, TriStar2S LB 942, Germany) with an excitation wavelength of 355 nm and an emission wavelength of 460 nm. The HIS release rate was calculated as a percentage compared to the model group:

Release ratio (%) = (C or M or T – B) / (M – B) × 100%, where B, C, M, and T represented the same as those in Measurement of *β*-HEX.

Toluidine blue staining

RBL-2H3 cells were seeded and cultured into a 6-well culture plate on a cell climbing slice overnight. The cells were treated with different concentrations of benzoylpaeoniflorin (**5**) (5, 25, 100 μmol·L^{-1}) and anti-DNP-IgE with a final concentration of 750 ng·mL^{-1}. The method of anti-anaphylaxis model was followed. Then, the slice was immediately placed in 95% ethanol. Subsequently, toluidine blue staining solution was added. The cell morphology was observed under a microscope (CARL ZEISS-Axio Ver AI, Germany).

F-actin microfilament staining

RBL-2H3 cells were treated the same as toluidine blue staining before stained by TRITC Phalloidin (100 nmol·L^{-1}). F-actin microfilament staining was performed according to the instruction manual. Finally, the cytoskeletons were examined under an inverted confocal fluorescence microscope (CARL ZEISS-Axio Ver AI, Germany) equipped with TRITC excitation/emission filter (E_x/E_m = 540/570 nm) and DAPI excitation/emission filter (E_x/E_m = 364/454 nm).

Mitochondrial membrane integrity

RBL-2H3 cells were seeded and cultured into a 6-well culture plate. Then, the cells were treated the same as toluidine blue staining before stained using 1 μg·mL^{-1} of rhodamine 123. The fluorescence of rhodamine was observed with excitation and emission wavelengths at 488 and 530 nm.

Assessment of IL-3, IL-4, IL-5, and IL-13 production

RBL-2H3 cells were seeded and cultured into a 24-well culture plate overnight. The cells were treated with different concentrations of benzoylpaeoniflorin (**5**) (5, 25, and 100 μmol·L^{-1}) and anti-DNP-IgE at a final concentration of 750 ng·mL^{-1}. The method of anti-anaphylaxis model was followed to collect the supernatant. The levels of IL-3, IL-4, IL-5, and IL-13 in the supernatant were measured by ELISA kits (Jingmei Biological Technology, Jiangsu, China), according to the manufacturer's instructions.

Western blot analysis

Western blot was used to analyze the changes in protein expression before and after drug incubation. After incubated with the compounds, cells were lysed in the radio-immunoprecipitation assay lysis buffer (RIPA; Sigma, MO, USA) for 30 min under the ice-old condition. A BCA protein assay kit (Invitrogen, Grand Island, NY) was used to measure the protein concentrations. The primary antibodies (CST, MA, USA) were anti-p38 (1 : 1000), anti-phospho-p38 (1 : 1000), anti-ERK (1 : 1000); anti-phospho-ERK (1 : 1000), anti-JNK (1 : 1000), anti-phospho-JNK (1 : 1000) and anti-*β*-actin (1 : 1000). Blots were further incubated with anti-rabbit IgG-horseradish peroxidase-conjugate antibody (Abcam, Cambridge, UK) at a 1 : 2000 dilution at room temperature for 1 h. Blots were visualized using Image Quant ™ LAS 4000 Luminescent image analyzer (Fujifilm Life Science, Tokyo, Japan). ImageJ was employed for densitometric analysis.

Molecular docking simulation

The crystal structures of HDC (PDB code: 4E1O), ERK (PDB code: 5UMO) (with respect to the high homology between ERK1 and ERK2, we extracted the structure of ERK2 for analysis), p38 (PDB code: 4LOO), and JNK1 (PDB code: 4LOO) were obtained from Protein Data Bank. Before the docking process, the structure of the protein was treated by adding hydrogen atoms, deleting water molecules, assigning AMBER7 FF99 charges, and a 100-step minimization process using Sybyl X_2.1. The molecular structure was generated with the Sybyl/Sketch module and optimized using Powell's method with the Tripos force field with the convergence criterion set at 0.005 kcal/(Å mol) and assigned charges with the Gasteiger-Hückel method. Other docking parameters were kept to the default values. Molecular docking was carried out *via* the Autodock.

IgE-mediated passive cutaneous anaphylaxis (PCA) in BALB/c mice

The assay was performed as previously reported with some modifications [5]. Five-week-old male BALB/c mice were kept on a 12 h-light/-dark cycle at 23 ± 3 °C with 55% ± 15% relative humidity. They were given standard laboratory rodent chow and water. After acclimatized for one week, the mice were randomly divided into the following five groups based on body weight: a control group (not sensitized), a model group (DNP-BSA antigen-treated IgE group), and treatment groups [benzoylpaeoniflorin (**5**)/DNP-BSA-treated IgE group]. The experimental protocols for BALB/c mice were approved by the Ethics Committee for Experimental Animals of Beijing Union-Genius Medical Technology Development Co., [permit number: 2019-002 (research)]. The animals were housed in the Animal Center of Beijing Union-Genius Medical Technology Development Co.. These facilities achieved accreditation (1438#) from the Association for Assessment and Accreditation of Laboratory Animal Care International (AAALAC International), and animals were maintained according to the 'Guide for the Care and Use of Laboratory Animals' (National Research Council, 2011).

Experimental protocol for the IgE sensitization and antigen challenge of mice was shown in Figure S2 (Supporting Information). Mice were passively sensitized for 24 h through intradermal administration of anti-DNP-IgE into the left ear (0.75 μg in 15 μL). Different concentrations of benzoylpaeoniflorin (**5**) solution was orally administrated to IgE-sensitized mice one hour before DNP-BSA antigen challenge. The DNP-BSA was injected *via* the tail vein (250 μg in 200 μL 0.4% Evans blue). Control mice were sensitized and chal-

lenged with normal saline as a DNP-BSA vehicle. After observation for 30 min, the left ears were cut into pieces and put in 800 μL of acetone-normal saline (7 : 3) solution at 65 °C for 12 h. After centrifugation for 15 min (3000 rpm·min^{-1}, 4 °C), 200 μL of supernatant was added into a new 96-well plate. Absorbances were measured at 620 nm by a microplate reader (Berthold, TriStar2S LB 942, Germany).

Statistical analysis

Data are presented as mean ± SD. All data were analyzed using a one-way analysis of variance (ANOVA), followed by Tukey's tests. Graph Pad Prism® software (GraphPad Software, La Jolla, CA, USA) was used to draw graphs and for statistical analysis. The symbol * indicated a significant difference with the control group, $^{*}P < 0.05$, while the symbol # indicates a significant difference with the model group, $^{\#}P < 0.05$.

Results

Bioactivity-guided isolation of the fractions of P. lactiflora extract

The *in vitro* cytotoxicity and inhibitory activity against *β*-HEX and HIS of fractions CS-3, CS-4, CS-5, and CS-6 were determined on DNP-BSA stimulated RBL-2H3 cells. It showed that CS-4 fraction exhibited stronger activity by reducing the release of *β*-HEX and HIS with higher cell survival rates, ranging from 0.2–20 μg·mL^{-1} (Fig. S1, Supporting Information). It is reasonable to suggest that CS-4 might represent the active fraction. Afterwards, CS-4 was subjected to repeated column chromatography over Sephadex LH-20, RP-18, and silica gel, and semipreparative HPLC to get eighteen cage-like monoterpenoid glycosides (**1**−**18**) (Fig. 1; Table S1, Supporting Information).

Cytotoxic effect and β-HEX and HIS inhibition ability of compounds (1−18)

In order to evaluate the cytotoxicity of all compounds, MTT assay was performed on DNP-BSA stimulated RBL-2H3 cells. Except for compounds **10** and **18**, the remaining compounds exhibited little/none cytotoxic effects with IC_{50} > 100 μmol·L^{-1} (Table 1). Afterwards, the ability of compounds (**1**−**18**) to inhibit the releasement of *β*-HEX and HIS were measured. Results show that compounds **1**, **5**, **6**, **11**, **12**, **15**, and **17** significantly reduced the release rate of *β*-HEX

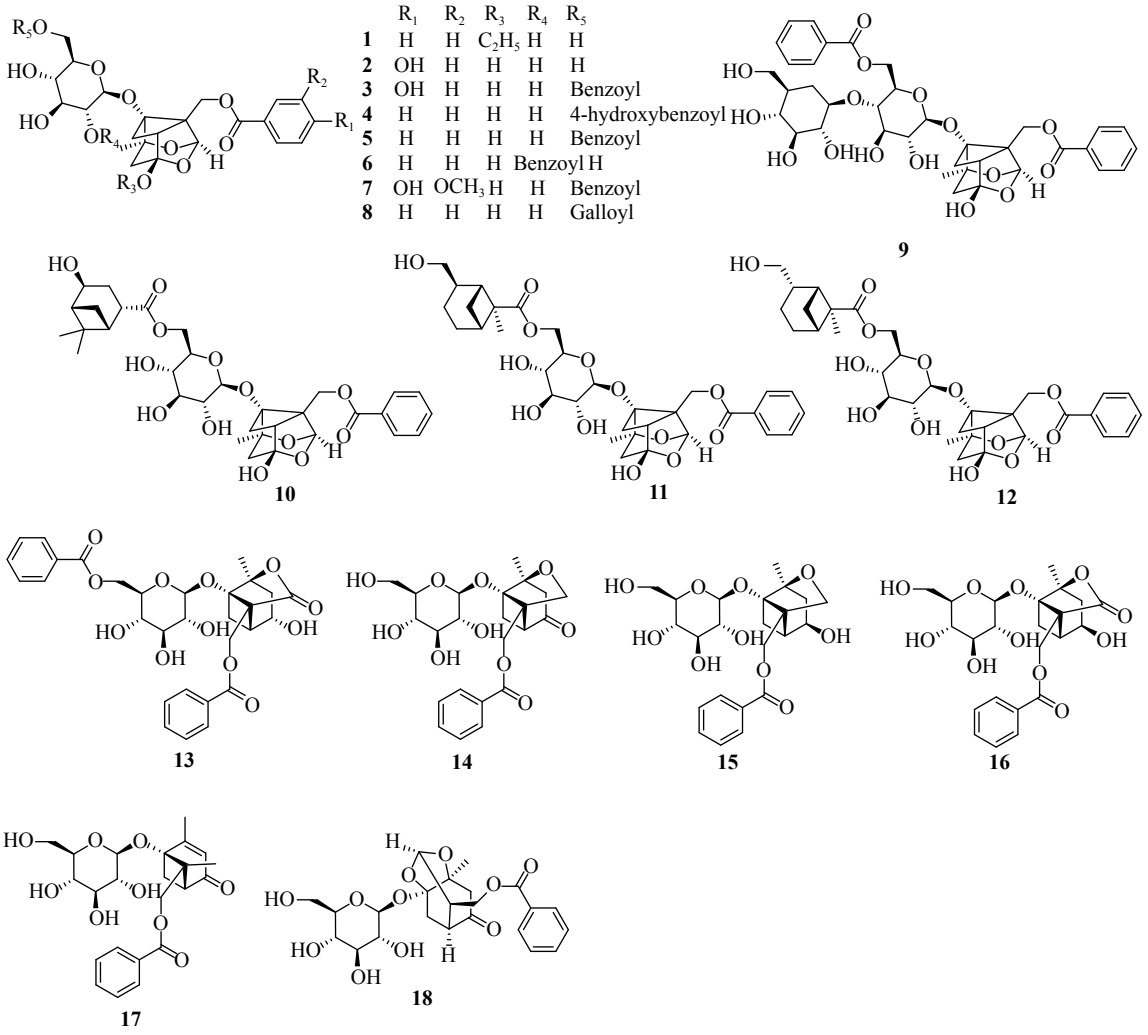

Fig. 1 Structure of compounds 1−18

Table 1 Cytotoxic effect and inhibition ability of compounds 1–18 on DNP-SBA-stimulated RBL-2H3 cells

No.	IC_{50} (μmol·L^{-1})	EC_{50} (μmol·L^{-1})	
	cytotoxicity	*β*-HEX	HIS
1	> 100	67.47 ± 9.11	55.20 ± 8.66
2	> 100	> 100	67.06 ± 3.40
3	> 100	86.38 ± 4.60	> 100
4	> 100	> 100	> 100
5	> 100	6.34 ± 1.14	18.06 ± 2.10
6	> 100	36.93 ± 4.01	30.54 ± 1.55
7	> 100	> 100	> 100
8	> 100	40.39 ± 4.60	> 100
9	> 100	> 100	> 100
10	80.33 ± 0.12	84.87 ± 10.66	55.45 ± 8.62
11	> 100	61.01 ± 6.84	77.26 ± 11.18
12	> 100	55.70 ± 6.71	55.29 ± 5.55
13	> 100	> 100	> 100
14	> 100	> 100	> 100
15	> 100	79.68 ± 10.83	68.28 ± 6.49
16	> 100	> 100	60.51 ± 5.53
17	> 100	60.52 ± 5.36	77.56 ± 10.70
18	48.16 ± 2.54	89.62 ± 6.23	87.02 ± 7.32

and HIS compared with the model group (Table 1). Benzoylpaeoniflorin (**5**) might exert a strong effect on anti-anaphylaxis, because it inhibited the production of HIS and *β*-HEX at very low concentrations *in vitro* (Fig. 2), with EC_{50} values of 6.34 ± 1.14 and 18.06 ± 2.10 μmol·L^{-1}, respectively. Therefore, benzoylpaeoniflorin (**5**) was selected for mechanism study.

Inhibitory effect of activation of HDC

The result of "Chi-Shao" extracts reducing the release rate of HIS inspired us to hypothesize potential anti-anaphylactic activity possibly by direct interaction with the HDC molecule. To verify the effect of "Chi-Shao" extract on HDC activity, we established a microbiological model of *Klebsiella pneumonia*, where HCD was highly expressed to catalyze L-histidine converting HIS. Benzoylpaeoniflorin (**5**) were chosen to evaluate their inhibitory efficiency on HDC activity. Preliminary results proved the evidence of our hypothesis after 24 h of incubation in a dose of 5, 25, and 100 μmol·L^{-1} compared to the control group. We found that benzoylpaeoniflorin (**5**) inhibited HIS by up to 50% at the high concentration of 100 μmol·L^{-1} (Fig. 3). This finding indicated that benzoylpaeoniflorin (**5**) is a potential HDC inhibitor.

Effects on cytokine generation in antigen-stimulated RBL-2H3 mast cells

Except of *β*-HEX and HIS, proinflammatory cytokines

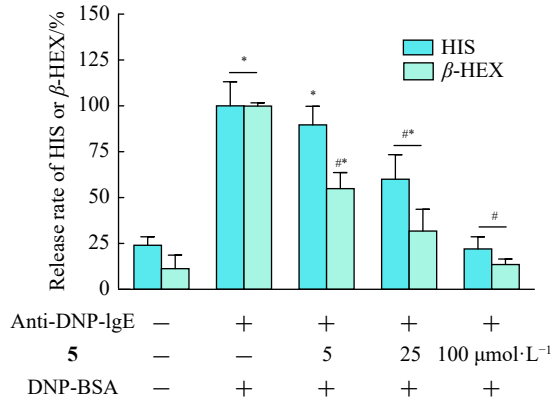

Fig. 2 Effects of compound 5 on the levels of *β*-HEX and HIS in DNP-SBA-stimulated RBL-2H3 cell model. Data are expresed as mean ± SD of three independent experiments. The symbol * indicates significant difference with the control group, $^{*}P < 0.05$. The symbol # indicates significant difference with the model group, $^{\#}P < 0.05$

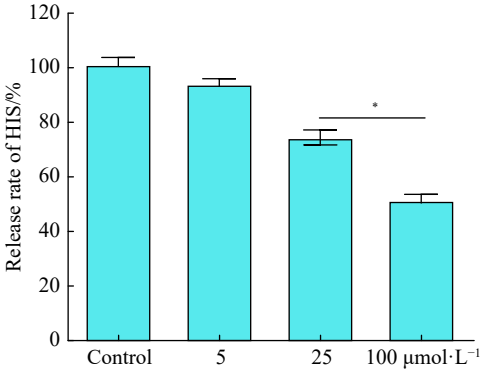

Fig. 3 Effect of compound 5 on the levels of HIS in *Klebsiella pneumonia* model. Data are expressed as mean ± SD of three independent experiments. The symbol * indicates significant difference with the control group, $^{*}P < 0.05$

including IL-3, IL-4, IL-5 and IL-13, are important markers of mast cell degranulation in RBL-2H3 cells. We first observed the degranulation morphology on RBL-2H3 cells stained by Toluidine blue (Fig. 4). The model group showed obvious degranulation, with most of the cell membranes being broken, leading to incomplete cell structure. For the treatment group, the severity of cell degranulation gradually decreased after treatment with the concentration gradient of 5, 25, 100 μmol·L^{-1} of benzoylpaeoniflorin (**5**), suggesting that it has the potential of inhibiting RBL-2H3 cells degranulation. Meanwhile, in the ELISA assay, we observed that pretreatment with benzoylpaeoniflorin (**5**) markedly downregulated the overproduction of IL-3, IL-4, IL-5, and IL-13 (5, 25, and 100 μmol·L^{-1}) compared with the control group (Figs. 5A, 5B, 5C, 5D). Cytoskeletal rearrangement is a key step in the degranulation process [6]. Phalloidin can selectively bind to filamentous actin (F-actin) with a high affinity in cells [7]. We observed severely changed cytoskeleton (uncompleted edges, jagged sides and curled cytoskeletons) on DNP-BSA stimulated RBL-2H3 cells through F-actin micro-

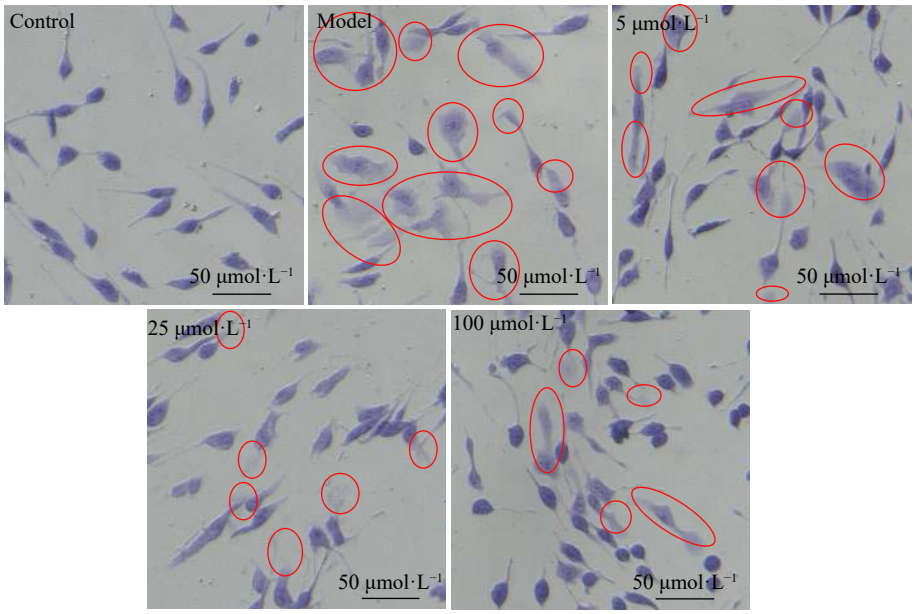

Fig. 4 Microscopic analysis of compound 5 pre-incubation on degranulation in response to DNP-BSA stimulation

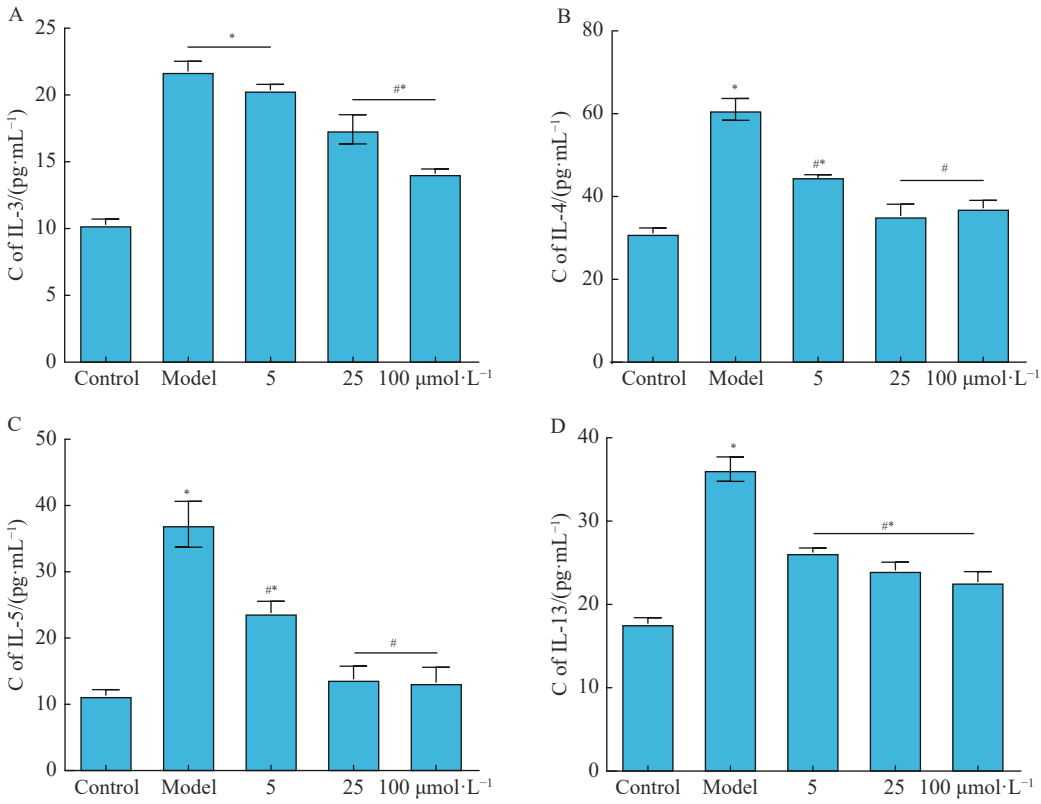

Fig. 5 Effects of compound 5 on the levels of IL-3 (A), IL-4 (B), IL-5 (C) and IL-13 (D) in DNP-SBA-stimulated RBL-2H3 cells model. Data are expressed as mean ± SD of three independent experiments. *$P < 0.05$ *vs* control. #$P < 0.05$ *vs* model

filament staining (Fig. 6). However, the destroyed cytoskeleton was gradually repaired after treatment with benzoylpaeoniflorin (**5**) (5, 25, 100 μmol·L^{-1}). We clearly observed that the cytoskeleton became normal at the concentration of 100 μmol·L^{-1}. The mitochondrial ultrastructural changes are also involved in anaphylactic reactions. It has been reported that inflammatory factors cause changes in mitochondrial membrane potential leading to changes in permeability [8, 9]. Thus, the effect of benzoylpaeoniflorin (**5**) on the integrity of the mitochondrial membrane was examined by fluorescence

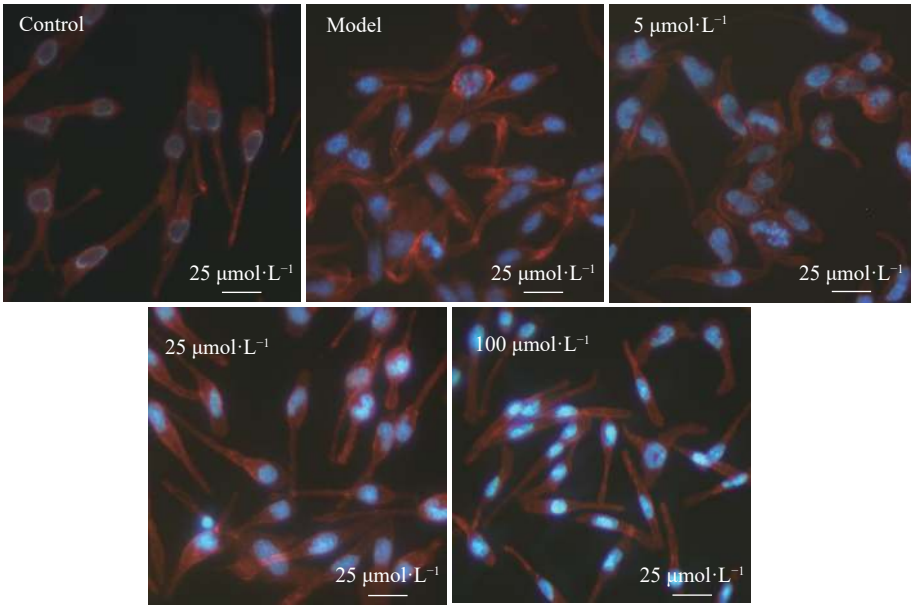

Fig. 6 Protective effects of compound 5 on the cytoskeletal in DNP-SBA-stimulated RBL-2H3 cell model

rhodamine dye imaging. The model group showed unclear fluorescence indicating that the mitochondria were damaged in DNP-BSA stimulated RBL-2H3 cells (Fig. 7). Inspiringly, benzoylpaeoniflorin (**5**) amended the insult of DNP-BSA on mitochondrial membrane at a relatively low concentration (25 μmol·L^{-1}). The above results indicate that benzoylpaeoniflorin (**5**) can repair the damage of cytoskeletal and mitochondrial membrane caused by anaphylactic reactions *in vitro*, which also indicates a reduction in cytokine.

Sequence and structure alignment among HDC and MAPKs

IgE-mediated anaphylaxis reaction can produce proinflammatory cytokines through activation of the MAPK signaling pathway. Considering that benzoylpaeoniflorin (**5**) may simultaneously inhibit HDC activity and MAPK pathway, we first extracted the amino acid sequences of HDC and ERK2, JNK, and p38 from NCBI database, and compared each of them using the software BLAST (Basic Local Alignment Search Tool, which is freely available at https://blast.ncbi.nlm.nih.gov/Blast.cgi). Finally, we used the software Sequence & Structure Alignment (available through Web interface at https://www.rcsb.org/#Category-analyze) to visualize and compare the models obtained.

We found that HDC shared 54.55% sequence identities with ERK, 32.61% JNK, and 35.71% p38, respectively (Table S2, Supporting Information). However, we have not obtained lower E value. Therefore, their homology existed more accidental factors. Furthermore, concerning three-dimensional structures, the portion of the enzyme-catalyzed site of HDC overlaps with the ATP-binding pockets of MAPKs (Fig. 8), which is a good illustration of the dual inhibitory effect of benzoylpaeoniflorin (**5**).

Effects on the activation of MAPK pathway in activated RBL-2H3 cells

The result of sequence and structure alignment among HDC and MAPKs inspired us to hypothesize that benzoylpaeoniflorin (**5**) down-regulated inflammatory cytokines, possibly by combining the ATP pockets of MAPKs and cutting their phosphorylation accordingly. Western blot analysis showed that the levels of P-p38, P-ERK1/2, and P-JNK in the model group significantly increased in RBL-2H3 cells compared with the control group. However, after the cells were incubated with benzoylpaeoniflorin (**5**), the phosphorylation levels markedly decreased compared with the model group (Figs. 9A, 9B).

The results of molecular docking

In order to gain a deep insight of the binding behavior of benzoylpaeoniflorin (**5**) to HDC and MAPKs from the view of ligand-enzyme interactions, molecular docking simulations were performed by AutoDock with a crystal structure of HDC, ERK, JNK, and p38 using a previous reported crystal structure. The results showed that the binding energy between benzoylpaeoniflorin (**5**) and proteins was very low, indicating that benzoylpaeoniflorin (**5**) tightly binds with target proteins (Table S3, Fig. S3). As shown in Fig. 10A, benzoylpaeoniflorin (**5**) bound well to HDC and occupied the enzyme catalytic site, incurring that L-histidine cannot be catalyzed to HIS. Meanwhile, benzoylpaeoniflorin (**5**) was well-docked into ERK, p38, and JNK at the ATP binding site (Figs. 10B, 10C, 10D). The binding mode of benzoylpaeoniflorin (**5**) in the active pockets all matched the classical binding mode of occupying active pocket-based ERK, p38, and JNK inhibitors. Moreover, the C4-OH and glycosyl moiety of benzoylpaeoniflorin (**5**) formed more and strong hydrogen bonds interaction with the amino acid residues of MAPKs at the ATP active sites (Fig. S3). The benzoyl part fit well into the active pocket sharing hydrophobic interaction. The perfect binding modes reasonably explain the significant inhibitory activities of benzoylpaeoniflorin (**5**) against HDC and ERK,

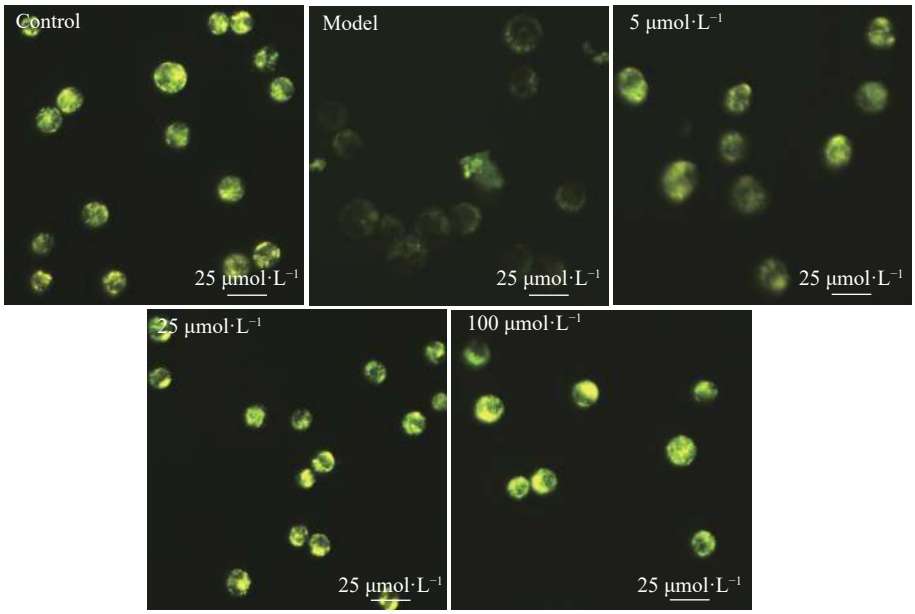

Fig. 7 Protective effects of compound 5 on mitochondrial membrane in DNP-SBA-stimulated RBL-2H3 cells model

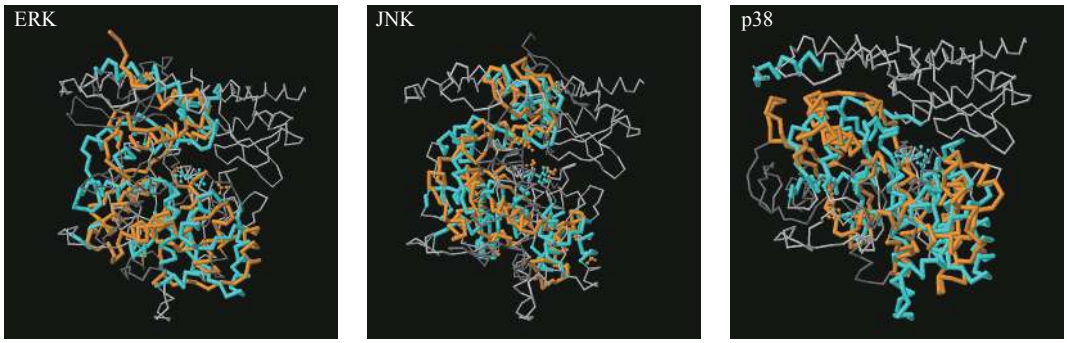

Fig. 8 Molecular models of HDC overlaping MAPKs. Cyans, yellow and gray indicate chemically similar amino acids of HDC, chemically similar amino acids of MAPKs, and chemically dissimilar (non homologous) amino acids, respectively

JNK, and p38 kinase.

Effects of benzoylpaeoniflorin (5) on the passive cutaneous anaphylaxis in mice

We also evaluated the anti-anaphylactic activity of benzoylpaeoniflorin (**5**) *in vivo* on PCA using BALB/c mice. PCA is a widely used *in vivo* model to investigate the anaphylactic response [10]. The vascular permeability of ears in the model group greatly increased. After oral administration of benzoylpaeoniflorin (**5**) to mice, the leakage of the Evans blue dye from ears decreased (Figs. 11A, 11B). This suggested that benzoylpaeoniflorin (**5**) suppressed the IgE-mediated PCA reaction in antigen-challenged mice.

Discussion

Allergy, also known as allergic diseases, is considered as a disorder of the immune system when a person is exposed to typically harmless substances in the environment. These diseases include hay fever, food allergy, atopic dermatitis, allergic asthma, and anaphylaxis [11-13].

Anaphylaxis is a serious allergic reaction that is rapid in onset and may cause death. Anaphylactic reaction is also known as type I hypersensitivity reaction, which will occur when the bodies are contact with the same antigen again. Allergens in nature are diverse, for example, fungi, insects, pollens, animal hair, certain food or dust mites are all very common allergens. After being stimulated by an antigen, the IgE is produced by specific B cells binding to FcεRI rapidly, and a functional connection between the allergen and the effector cells was set up [14, 15]. It has been reported that the protection mechanisms of anti-anaphylaxis drugs may be from the following three ways: 1) inhibiting the release rate of biologically active media; 2) antagonizing the symptoms of anaphylactic reactions; and 3) reducing the effector reactivity [16].

Paeonia lactiflora roots are commonly used components of traditional medicine in Northeast Asia and possess various beneficial properties, including anti-inflammatory, anti-cancer, anti-anaphylactic, anti-oxidant, anti-diabetic activity, and liver protection. Over the past two decades, many constituents have been isolated from the roots of *P. lactiflora*, which have been found to feature a broad range of the above biological activities. Nonetheless, the bioactive constituents and underlying mechanisms of its anti-anaphylactic effect are

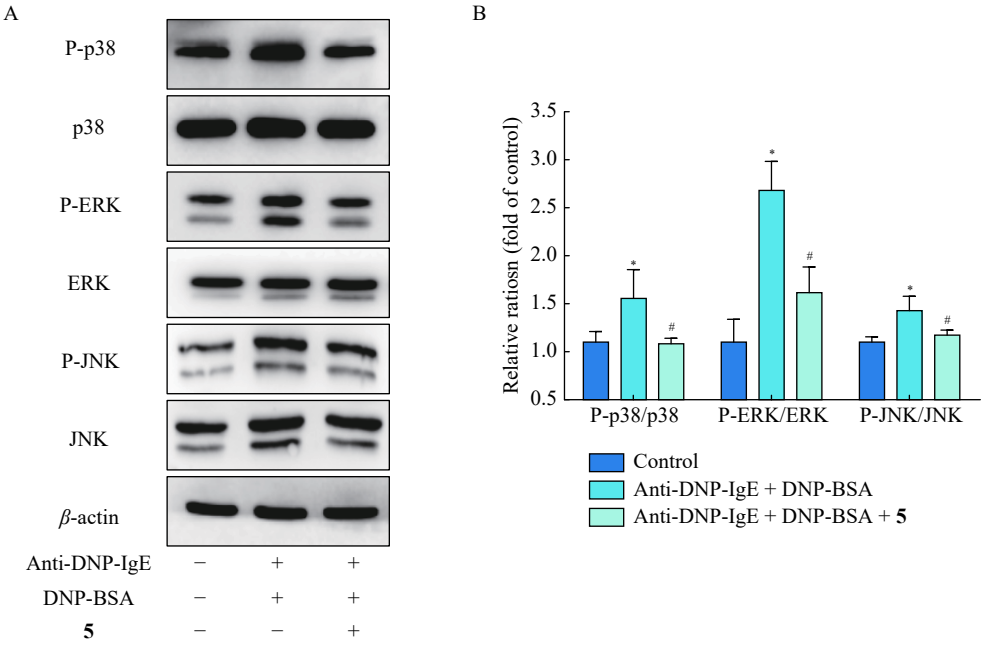

Fig. 9 Effects of compound 5 on regulation of p-MAPKs/MAPKs in RBL-2H3 cells. (A) The levels of p-MAPKs/MAPKs were analyzed by Western blot; (B) Calculated. Data are expressed as mean ± SD of three independent experiments. $^{*}P < 0.05$ *vs* control. $^{\#}P < 0.05$ *vs* model

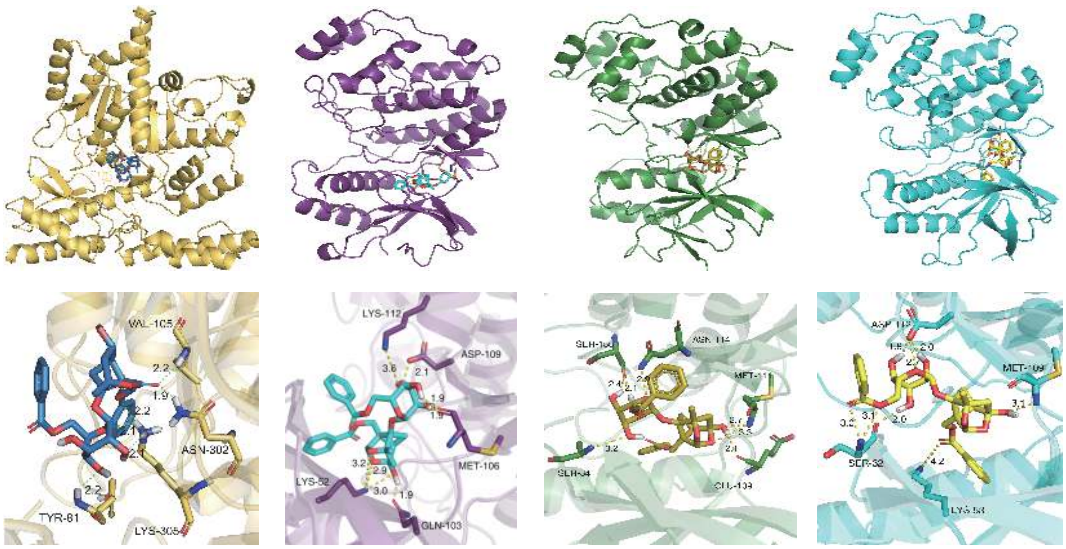

Fig. 10 Binding mode of compound 5 with proteins. (A) HDC; (B) ERK; (C) JNK; and (D) p38

poorly understood.

In this study, anti-anaphylactic assay on IgE-mediated degranulation in RBL-2H3 cells was firstly employed for bioactivity-guided fractionation of *P. lactiflora*, resulted in the discovery of 18 cage-like monoterpenoid glycosides (**1**−**18**) from the bioactive fraction. We observed that seven compounds (**1**, **5**, **6**, **11**, **12**, **15**, and **17**) were hit in the anti-anaphylaxis assay on mast cell degranulation in RBL-2H3 cells, which down-regulated HIS and *β*-HEX at the meaningful concentrations (EC_{50} < 100 μmol·L^{-1}) with low cytotoxicity. Especially, benzoylpaeoniflorin (**5**) showed the most potent inhibition of HIS and *β*-HEX, with EC_{50} values of 6.34 ± 1.14 and 18.06 ± 2.10 μmol·L^{-1}, respectively. Therefore, benzoylpaeoniflorin (**5**) was selected as the prioritized compound for the study of action of mechanism.

HDC genes are sensitive for anaphylactic diseases, and their expression affect the severity of anaphylaxis symptoms [17]. Hence, targeting HDC may decrease the production of histamine and produce anti-anaphylaxis reaction activity [18]. In addition, anti-anaphylactic drugs targeting HDC have not been available on the market. We observed that cage-like monoterpene glycosides significantly reduced the release rate of HIS in the IgE-mediated hypersensitivity model on RBL-2H3 cells. It inspired us to hypothesize that it is pos-

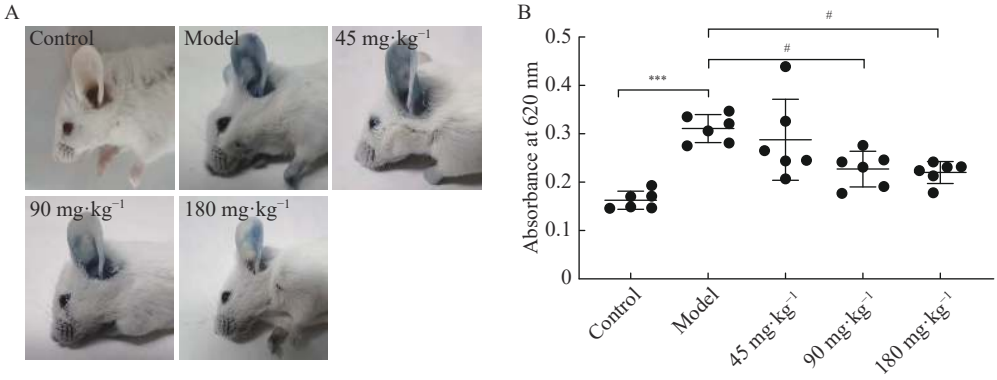

Fig. 11 Effects of compound 5 on the passive cutaneous anaphylaxis in mice. (A) The representative photographic images of ears; (B) Absorbance values. Data are expressed as mean ± SD (n = 6/group). $^{\#}P < 0.05$, $^{\#\#}P < 0.01$ *vs* model group, $^{***}P < 0.001$ *vs* the control group

sible to target HDC. We found that benzoylpaeoniflorin (**5**) inhibited HIS by up to 50% at high concentrations on the microbiological model of *Klebsiella pneumonia*. Recently, such methods have been reported to screen HDC inhibitors due to high HDC expression in *Klebsiella pneumonia* [19].

In the early phase inflammatory reaction, the MAPK signaling pathway can be activated to produce inflammatory cytokines, including IL-3, IL-4, IL-5, and IL-13, etc. Those mediators maintain the anaphylactic reactions, and in turn reactivate much early phase inflammatory reaction. Therefore, inhibiting the release of inflammatory cytokines is a target for the development of drugs for anaphylaxis reaction. In our study, pretreatment with benzoylpaeoniflorin (**5**) markedly inhibited the overproduction of IL-3, IL-4, IL-5, and IL-13 compared with the DNP-BSA-treated model group. We first performed Sequence & Structure Alignment among HDC and MAPKs, which showed that the portion of the enzyme-catalyzed site of HDC overlaped with the ATP-binding pockets of MAPKs. This finding indicated the possibility of benzoylpaeoniflorin (**5**) dual targeting HDC and MAPKs. In our further Western blot assay, the effects on down-regulating inflammatory cytokines of benzoylpaeoniflorin (**5**) were proved by combining the ATP pockets of ERK1/2, JNK, and p38 to reduce their phosphorylation accordingly.

Moreover, we employed a molecular docking approach to examine the prospective interaction between benzoylpaeoniflorin (**5**) and HDC and MAPKs. The results showed that benzoylpaeoniflorin (**5**) occupied the enzyme catalytic site of HDC to block L-histidine to be catalyzed. Meanwhile, benzoylpaeoniflorin (**5**) was well-docked into ERK, p38, and JNK to compete for the ATP pockets with ATP, leading to decreases in phosphorylation level.

Finally, the effect of benzoylpaeoniflorin (**5**) on the passive cutaneous anaphylaxis *in vivo* was enforced on PCA using BALB/c mice. PCA is a local cutaneous reaction, quickly leading to capillary dilation and increased the vascular permeability, which can be seen by infiltrating the reaction sites. The result showed benzoylpaeoniflorin (**5**) suppressed the IgE-mediated PCA reaction in antigen-challenged mice.

Conclusion

The present study demonstrated that cage-like monoterpenoid glycosides have better anti-anaphylaxic effects with less cytotoxic effects. In addition, the representative benzoylpaeoniflorin (**5**) has been shown to reduce HIS release through binding to HDC and to inhibit the release of inflammatory factors through blocking ERK1/2, JNK, and p38 in the MAPK signaling pathway. It is also of great significance that benzoylpaeoniflorin (**5**) can repair cytoskeletal and mitochondrial membrane damage caused by anaphylactic reactions. Molecular docking simulations have provided a deep insight of the inhibitory behavior of benzoylpaeoniflorin (**5**) from the view of ligand-enzyme interactions. Besides, benzoylpaeoniflorin (**5**) exhibits the anti-anaphylactic effect on PCA using BALB/c mice. Thus, our findings demonstrate that cage-like monoterpenoid glycosides from *P. lactiflora* can be considered as promising HDC and MAPK signaling pathway dual-inhibitors of natural origin, which may guide the discovery and development of potent drug against anaphylactic reaction.

Abbreviations: IgE, serum immunoglobulin E; RBL, rat basophil leukemia; β-HEX, β-hexosaminidase, HIS, histamine; IL, interleukin; pre-HPLC, preparative High Performance Liquid Chromatography; p-ERK1/2, phosphorylated extracellular signal-regulated kinase, p-JNK, phosphorylated c-Jun N-terminal kinases; p-p38, phosphorylated p38 mitogen-activated protein kinase; HDC, histidine decarboxylase; MAPKs, mitogen-activated protein kinase family proteins.

Supplementary materials

Supplementray information can be acquired by e-mail to corresponding author.

References

[1] Sicherer SH, Furlong TJ, Munoz-Furlong A, *et al*. A voluntary registry for peanut and tree nut allergy: characteristics of the first 5149 registrants [J]. *J Allergy Clin Immunol*, 2001, **108**(1): 128-132.

[2] Lin S, Cicala C, Scharenberg AM, *et al*. The FcεRIβ subunit functions as an amplifier of FcεRIγ-mediated cell activation

signals [J]. *Cell*, 1996, **85**(7): 985-995.
[3] Li R, Zhang JF, Wu YZ, *et al*. Structures and biological evaluation of monoterpenoid glycosides from the roots of Paeonia lactiflora [J]. *J Nat Prod*, 2018, **81**(5): 1252-1259.
[4] He CN, Peng Y, Zhang YC. Phytochemical and biological studies of Paeoniaceae [J]. *Chem Biodivers*, 2010, **7**(4): 805-838.
[5] Nishi K, Teranishi M, Yasunaga S, *et al*. The major whey protein *β*-lactoglobulin inhibits IgE-mediated degranulation of RBL-2H3 cells and passive cutaneous anaphylaxis in mice [J]. *Int Dairy J*, 2014, **39**(1): 89-95.
[6] Fu M, Fu S, Ni S, *et al*. Inhibitory effects of bisdemethoxycurcumin on mast cell-mediated allergic diseases [J]. *Int Immunopharmacol*, 2018, **65**: 182-189.
[7] Chong YJ, Firdaus MN, Chean Hui AN, *et al*. Barrier protective effects of 2,4,6-trihydroxy-3-geranyl acetophenone on lipopolysaccharides-stimulated inflammatory responses in human umbilical vein endothelial cells [J]. *J Ethnopharmacol*, 2016, **192**: 248-255.
[8] Green DR, Lorenzo G, Guido K. Mitochondria and the autophagy-inflammation-cell death axis in organismal aging [J]. *Science*, 2011, **333**(6046): 1109-1112.
[9] Zheng W, Pan H, Wei L, *et al*. Dulaglutide mitigates inflammatory response in fibroblast-like synoviocytes [J]. *Int Immunopharmacol*, 2019, **74**: 105649-105657.
[10] Kim MJ, Kim YY, Choi YA, *et al*. Elaeocarpusin inhibits mast cell-mediated allergic inflammation [J]. *Front Pharmacol*, 2018, **9**: 591-600.
[11] Aam BB, Heggset EB, Norberg AL, *et al*. Production of chitooligosaccharides and their potential applications in medicine [J]. *Mar Drugs*, 2010, **8**(5): 1482-1517.
[12] Akdis M, Blaser K, Akdis CA. T regulatory cells in allergy: novel concepts in the pathogenesis, prevention, and treatment of allergic diseases [J]. *J Allergy Clin Immunol*, 2005, **116**(5): 961-968.
[13] Vo TS, Ngo DH, Kim SK. Gallic acid-grafted chitooligosaccharides suppress antigen-induced allergic reactions in RBL-2H3 mast cells [J]. *Eur J Pharm Sci*, 2012, **47**(2): 527-533.
[14] Kawa A. The role of mast cells in allergic inflammation [J]. *Respir Med*, 2012, **106**(1): 9-14.
[15] *Allergy and Allergic Diseases* [M]. Wiley-Blackwell, 2008.
[16] *Medical Immunology* [M]. People's Medical Publishing House, 2015.
[17] Nurul IM, Mizuguchi H, Shahriar M, *et al*. Albizia lebbeck suppresses histamine signaling by the inhibition of histamine H1 receptor and histidine decarboxylase gene transcriptions [J]. *Int Immunopharmacol*, 2011, **11**(11): 1766-1772.
[18] Bakrania AK, Patel SS. Combination treatment for allergic conjunctivitis-plant derived histidine decarboxylase inhibitor and H1 antihistaminic drug [J]. *Exp Eye Res*, 2015, **137**: 32-38.
[19] Hanieh H, Islam VIH, Saravanan S, *et al*. Pinocembrin, a novel histidine decarboxylase inhibitor with anti-allergic potential *in vitro* [J]. *Eur J Pharmacol*, 2017, **814**: 178-186.

Cite this article as: ZHONG Wan-Chao, LI En-Can, HAO Rui-Rui, ZHANG Jing-Fang, JIN Hong-Tao, LIN Sheng. Anti-anaphylactic potential of benzoylpaeoniflorin through inhibiting HDC and MAPKs from *Paeonia lactiflora* [J]. *Chin J Nat Med*, 2021, **19**(11): 825-835.